Seismic attenuation system for the AEI 10 meter Prototype

2012 Class. Quantum Grav. 29 245007

(http://iopscience.iop.org/0264-9381/29/24/245007)

Class. Quantum Grav. **29** (2012) 245007 (11pp) doi:10.1088/0264-9381/29/24/245007

Seismic attenuation system for the AEI 10 meter Prototype

A Wanner[1], G Bergmann[1], A Bertolini[2], T Fricke[1], H Lück[1], C M Mow-Lowry[1], K A Strain[1,3], S Goßler[1] and K Danzmann[1]

[1] Max Planck Institute for Gravitational Physics (Albert Einstein Institute), Leibniz Universität Hannover, Callinstr. 36, D-30167 Hannover, Germany
[2] National Institute for Subatomic Physics, Science Park 105, 1098 XG Amsterdam, The Netherlands
[3] Scottish University Physics Alliance, Institute for Gravitational Research, School of Physics and Astronomy, University of Glasgow, Glasgow G12 8QQ, UK

E-mail: alexander.wanner@aei.mpg.de

Received 16 August 2012, in final form 25 October 2012
Published 19 November 2012
Online at stacks.iop.org/CQG/29/245007

Abstract
Isolation from seismic motion is vital for vibration sensitive experiments. The seismic attenuation system (SAS) is a passive mechanical isolation system for optics suspensions. The low natural frequency of a SAS allows seismic isolation starting below 0.2 Hz. The desired isolation at frequencies above a few hertz is 70–80 dB in both horizontal and vertical degrees of freedom. An introduction to the SAS for the AEI 10 m Prototype, an overview of the mechanical design and a description of the major components are given.

PACS numbers: 04.80.Nn, 95.55.Ym

(Some figures may appear in colour only in the online journal)

1. Introduction to the seismic attenuation system

A prototype interferometer facility [1] is being set up at the Albert Einstein institute (AEI) in Hannover, Germany; a facility used for the purpose of development and testing of new techniques for the gravitational wave detector GEO 600 [2] and proposed third generation ground-based interferometric gravitational wave detectors, for example, the Einstein Telescope [3]. Further experiments, such as exploring quantum mechanical effects in macroscopic objects [4] and operating an interferometer below the standard quantum limit [5] are also being developed.

A large-scale ultra-high vacuum system has been built to isolate the facility from environmental noise sources such as acoustic and thermal fluctuations. The vacuum system consists of three walk-in tanks connected by vacuum tubes. Each of the three vacuum tanks is to be fitted with a seismically isolated optical table. These tables provide the mechanical

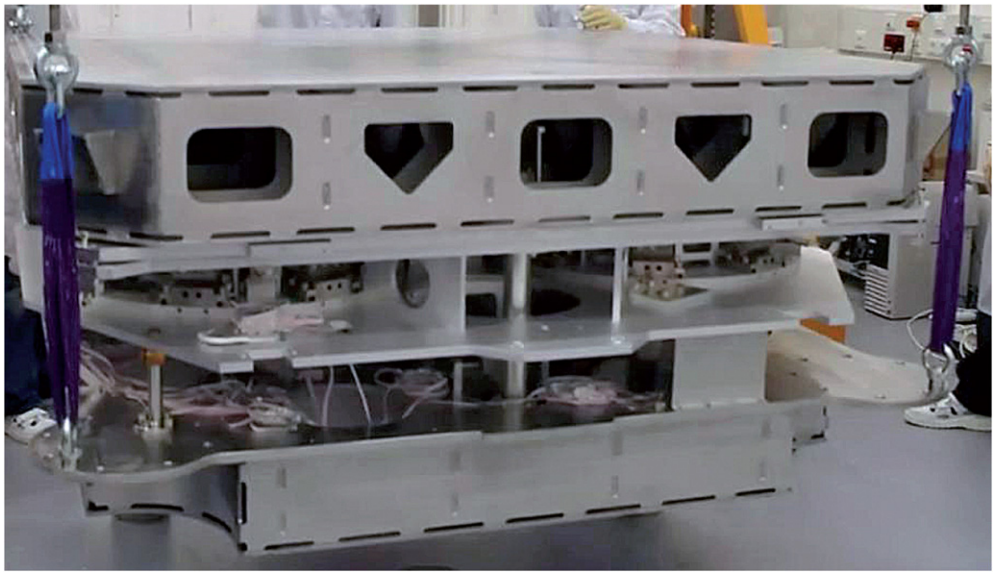

Figure 1. An AEI-SAS during installation into the vacuum system in March 2012. Triangular holes, visible in the table bench side, are isostatic supports for payload ballast rods. The spring box with geometric anti-spring (GAS) filters is the central part of the sandwich structure. An inverted pendulum (IP) leg is visible at the front. Details of these and other components are provided in the text.

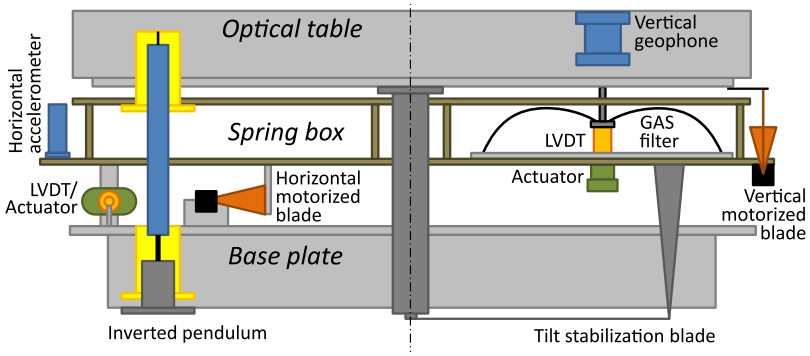

Figure 2. Schematic illustration of the seismic attenuation system (SAS), showing a side-on cutaway of the table. The main isolating elements (inverted pendulum (IP) legs, geometric anti-spring (GAS) filters), sensors (LVDTs, accelerometers and geophones), coil-magnet actuators and the horizontal motorized adjusters are present three times, spaced around the table on a centred circle at 120° from each other. For clarity, only one example of each of these is shown. The only exception are the four vertical motorized blades that are placed in each corner of the table. The other major components are a base plate which supports the SAS and is bolted to the ground, the spring box which is supported by the IP legs, and the optical table, supported by three GAS filters sandwiched in the spring box.

interface between the vacuum system and one or more multiple stage pendulum suspension systems [6] carrying the mirrors of the interferometer.

Each table is integrated with its supporting SAS, see figures 1 and 2. The specific custom design for the prototype is called the AEI-SAS. This design is derived from a prototype device,

the Horizontal Access Module—Seismic Attenuation System (HAM-SAS) developed by the California Institute of Technology for the gravitational wave detector Advanced LIGO [7]. These are six degree-of-freedom vibration isolators that shield the table from ground motion, the dominant environmental source of disturbance for experiments in the frequency range from 0.1 to 100 Hz. It was decided to apply a primarily passive approach to seismic isolation, in which a highly compliant spring system and the mechanical filtering properties of harmonic oscillators are employed. The AEI-SAS tables are designed to operate with natural frequencies as low as 0.05 Hz in horizontal and around 0.1 Hz in vertical degrees of freedom, allowing large vibration suppression ratios to be achieved. The AEI-SAS is designed to provide attenuation factors around 70–80 dB at a few Hz in vertical and horizontal directions along the main axes of the interferometer; preliminary measurements are given in [1]. An external injection bench (EIB-SAS), using identical isolating techniques as the AEI-SAS was built and tested at Nikhef for the Advanced VIRGO gravitational wave detector [8].

The passive system is paired with an active control system using co-located sensors and actuators to improve the attenuation performance, particularly near the fundamental resonances (rigid body modes) of the isolator, and at the lowest frequency resonances of the isolator structure. The AEI-SAS is damped by means of six independent single-input–single-output control loops, one for each translational (x, y, z) and rotational (*yaw*, *pitch*, *roll*) degrees of freedom defined such that for each table, x and y lie in a horizontal plane and are aligned to the main axes of the vacuum system, with z vertical.

Active isolation devices [9] make use of relatively stiff mechanics and sophisticated feedback strategy. Passive systems use the isolating properties of mechanical oscillators to attenuate seismic motion. In parallel, active controls are used to damp the fundamental rigid body modes at low frequencies using elementary control loops with low unity gain frequency. That makes the system insensitive to structural resonances of the payload, and consequently provides a robust solution that can be rapidly adjusted to accommodate the various experiments, planned for the AEI 10 m Prototype facility. Crosstalk between different suspension stages, to which a passive isolator is vulnerable, was not considered an issue because of very low mass ratio between the optical bench, which weighs about 1 tonne, and the freely suspended parts of the payload, which each weigh of order 100 g to 1 kg.

2. Mechanical design

The optical table of the AEI 10 m Prototype facility is a square-shaped stainless steel breadboard with side length 1750 mm, 400 mm thick, stiffened by an internal honeycomb web structure. The optical table rests on three vertical vibration isolators, the geometric anti-spring (GAS) filters [10], that provide mechanical compliance along the vertical degree of freedom, z, and in rotation around x and y. The three vertical isolators are sandwiched between rigid plates, forming the spring box (shown in figure 2), which is supported by three inverted pendulum (IP) legs. Tilt stabilization springs are installed to allow to stabilize tilt modes while maintaining a low vertical resonant frequency. Horizontal and vertical stoppers are used to pin the table at any defined position during the installation of optical components.

2.1. Vertical isolator: geometric anti-spring filter

The GAS filter is a tunable mechanical oscillator formed from flat elastic blades bent and radially compressed, as shown in figure 3. The blade pairs are radially compressed against each other, forming a crown of curved blades. The constrained radial stress creates an anti-spring effect that allows a very low effective stiffness to be achieved in the vertical direction.

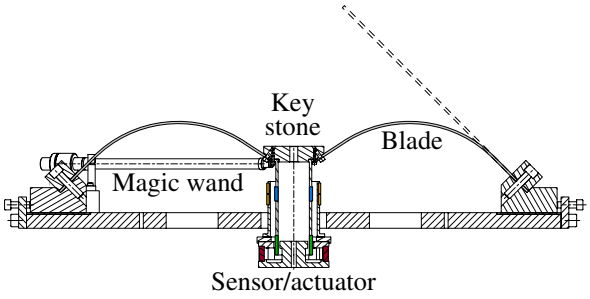

Figure 3. Cross-section of the geometric anti-spring (GAS) filter, showing vertical collocated sensor/actuator pair and one magic wand. The dashed line represents a relaxed blade before being stressed under load. The coloured blocks, representing windings of the coils and magnets (red), explained in figure 6.

The scientific payload is complemented by a set of ballast weights installed in the breadboard to achieve the floating load of the springs. Every piece of equipment placed on top of the table has to be weighed and the same amount of ballast removed to retain the same load in the system. The overall payload budget of each AEI-SAS is about 220 kg.

The effective elastic constant of the GAS filters can be tuned by mechanical adjustment of the compression of the blades, without changing their payload. Natural frequencies of a few tenths of a hertz can be obtained. Lower tuning can be achieved by applying positive feedback [11]. Each GAS filter was tuned separately to achieve a mechanical resonance frequency below 200 mHz at 320 kg nominal load. By adjusting the compression rate of the blades against the central keystone—the connection of all blades (see figure 3)—the filter reaches its nominal working elastic constant of 400 N m^{-1} at a resonant frequency of 180 mHz. At this tuning, the height changes 2 mm for a payload change of 100 g. The maximal vertical range is limited by end-stops at ± 5 mm. Further away from the working point the GAS filter compliance decreases substantially, because the GAS is a nonlinear device. The designed working point of 85 mm between the keystone's lower surface and the GAS filter plate's upper surface is used as a zero point setting for the vertical displacement measurement devices—the Linear Variable Differential Transformers (LVDT), see section 3.1. Each GAS filter incorporates one LVDT co-located with a voice-coil actuator below the keystone for position monitoring and feedback in vertical degree of freedom.

The inertia of the blades limits the vibration isolation power to -60 dB, forming an isolation plateau in the transfer function of the GAS filter, as shown in figure 4. This limiting effect is called centre-of-percussion effect. The isolation performance can be improved up to -80 dB by using add-on compensators, the so-called *magic wands* [12]. A counterweight at the end of the wand shifts the centre of percussion right on top of the effective pivot of the blades. To achieve maximal rigidity and minimal weight, silicon carbide proved to be a better material than aluminium, pushing the natural frequency of the wand assembly above 300 Hz.

Tilt stabilization. The vertical isolation stage of the AEI-SAS is composed of three GAS filters, which can be seen as parallel connected springs. The common mode of the three springs is the vertical motion of the table. The differential movement of the springs allows a rotation of the table surface about the x and y axes. The virtual pivot point of the tilt is located a few cm above the keystones and about 25–30 cm (depending on the payload configuration) below the plane of the centre of mass of the bench and payload. Therefore, the gravity induces a negative

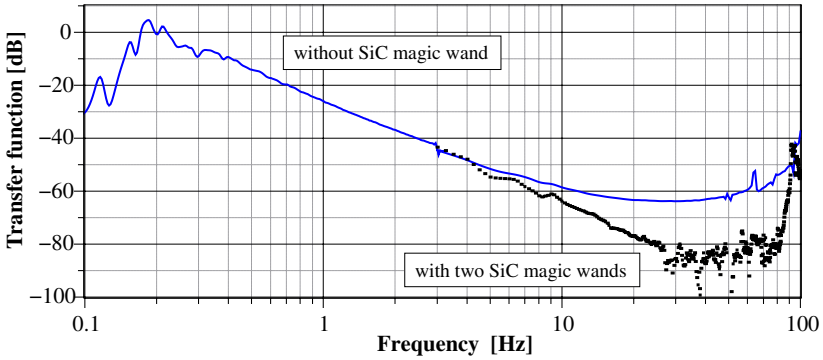

Figure 4. Performance of a single GAS filter with and without SiC magic wands measured in a vertical shaker test-stand without applying any active controls or damping. Above 30 Hz, the displacement transmitted through the GAS filter is below the resolution of the sensor, masking the true transfer function. The increase in the transfer function at high frequencies is assumed to be the flank of a group of resonances above 300 Hz produced by magic wands and GAS filter blades, which both can be damped with eddy-current dampers.

restoring torque that makes the system unstable. In order to independently adjust vertical and tilt stiffness, a tilt stabilization system made of an arm and three springs is installed below the optical table [13].

In the AEI-SAS, the blade springs are attached to the spring box, as shown in figure 2. The tip of each blade is connected by a tensioned wire to the arm. The stiffness of the blades adds a significant restoring torque between the optical table and the spring box. The tensioning of the springs at 44 N and the diameter of the wire were selected in order to raise the frequency of its first violin mode above 170 Hz.

2.2. Horizontal isolator: inverted pendulum

A three leg IP provides seismic isolation for horizontal translational (x, y) modes and for *yaw*. Each IP leg has two flexures, shown in figure 5: a short soft flexure on top and a stiff flexure on the bottom. The short top flexure serves as a hinge between the IP leg and the spring box. It allows the spring box plate to move in the horizontal plane constraining its *pitch* and *roll* movement. The bottom flexure provides the necessary restoring force for the table to keep the IP leg in the upright position [14]. Suitable sizing of the IP bottom flexure compensates for the gravitational torque on the verge of instability. The effective horizontal elastic constant κ_{eff} of the IP leg is basically the stiffness due to the bottom flexure, κ, reduced by the gravitational anti-spring constant, $\kappa_{\text{grav}} = \frac{mg}{L}$, produced by the mass load m of the IP:

$$\kappa_{\text{eff}} = \kappa - \frac{mg}{L}, \tag{1}$$

with length of the IP leg, L, and gravitational acceleration, g. Hence, the resonance frequency of the IP leg can be tuned by changing the payload mass.

The advantage of IP over conventional pendulums is the very low resonant frequency with a short pendulum length of 438 mm. The IP leg is an aluminium tube with 1 mm wall thickness, designed to reduce its weight and thereby its moment of inertia. The inertia of the legs limits the IP vibration transmissibility to −70 dB due to the centre-of-percussion effect [15]. The performance of the IP can be improved up to −90 dB, by adjusting the position of

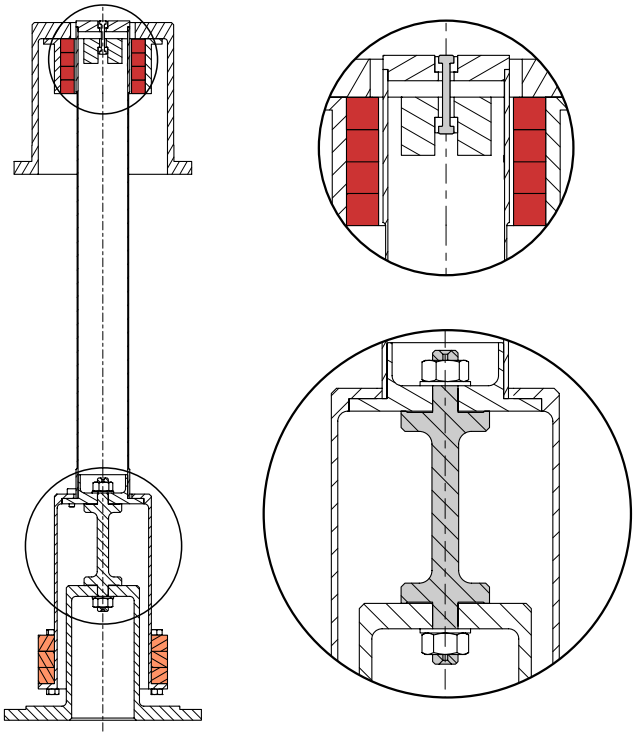

Figure 5. The inverted pendulum (IP) leg, with soft upper and stiff lower flexure (grey). Both flexures are machined from maraging steel. The magnets (red) for the eddy current damping of the leg's internal modes are distributed around the leg near the upper flexure. The lower bell supports balancing counterweights (orange) for fine tuning of the centre-of-percussion effect.

the centre of percussion, with the counterweights shown in figure 5. Internal resonances of the IP legs are damped by eddy-current dampers.

3. Sensors and actuators

The micro-seismic peak of the ground motion spectrum is close to the fundamental resonances of the AEI-SAS, and will excite the table into large-scale motion. To reduce this motion, the tables are equipped with a variety of sensors and actuators.

The sensors, subdivided in LVDTs and accelerometers/geophones, measure in different frequency bands. LVDTs measure the horizontal and vertical position of the table relative to the ground. Their frequency band ranges from static to 10 Hz. Accelerometers measure the acceleration of the spring box from 0.3 Hz up to 50 Hz. Placing the accelerometers on the spring box, which is constrained to move horizontally, reduces the accelerometer crosstalk with the angular noise. This allows to substantially lower the unity gain frequency of the inertial control improving the attenuation performance at low frequency where the angular noise dominates. Vertical geophones are attached to the breadboard to sense the vertical movement of the optical table.

Voice-coil actuators are used to perform modal damping and low-frequency positioning. These actuators drive the table relative to the ground. Stepper motors are used for fine

adjustments of the table position, thereby removing the static load from the voice-coil actuators, and for alignment.

3.1. Linear variable differential transformer

The position of the table is monitored by LVDTs. An LVDT is a non-contact measurement device with nanometre resolution and a dynamic range of tens millimetres [16]. LVDTs used in the AEI-SAS consist of two coaxial coils: a small primary excitation coil and a larger secondary sensing coil.

The excitation coil is driven by a sinusoidal signal at 15 kHz generating an alternating magnetic field. The sensing coil consists of two sets of windings, mounted and connected in series, but with opposed orientation. The excitation coil induces a signal proportional to displacement, when it slides between the two windings of the sensing coils. Thereby, the induced 15 kHz signal increases in one sensing winding, and decreases in the other.

The output is demodulated synchronously with the excitation source. The resulting rectified voltage is proportional to the displacement of the coil and its polarity indicates the direction of the displacement [17]. Over a total range of 6 mm the output of the horizontal and the vertical LVDT is linear within ± 0.2 % and ± 0.5 %, respectively, and has a resolution of 10 nm $\mathrm{Hz}^{-1/2}$.

3.2. Horizontal accelerometers

Accelerometers are used in the AEI-SAS to measure the horizontal inertial motion of the table and monitor the vibration isolation performance outside the control loop frequency band. The AEI-accelerometers are custom-made uniaxial devices machined with electric discharge machining from a single block of aluminium, and therefore called monolithic. The AEI-accelerometer mechanical design is similar to monolithic accelerometers used in TAMA-300 [18]. Newly designed corner-filleted flexures have been implemented to reduce the elastic restoring force and to increase the stress limitations during transport.

The test mass is suspended from a folded pendulum to reduce the natural frequency of the accelerometer while rigidly constraining its motion in a single direction to make it completely insensitive to all five orthogonal degrees of freedom. The folded pendulum geometry, a Watt-linkage [19], was originally proposed for this application and tested at the University of Western Australia [20].

A folded pendulum (see figure 7) consists essentially of a test mass with two hinging supports. The support at one end of the test mass is an ordinary pendulum with a positive restoring force. The other side of the test mass is supported by an IP contributing a negative restoring force. In this configuration, the positive gravitational spring constant of the ordinary pendulum is balanced by the negative gravitational spring constant of the IP. The residual elastic constant of the flexures is compensated by loading additional mass on the IP leg side [21]. Because of this design, the folded pendulum has a very low resonant frequency. The support geometry is such that all its soft flexures are in tension to eliminate buckling problems.

The AEI-accelerometers are tuned to 0.3 Hz resonance frequency. A miniaturized LVDT with reduced dynamic range and strongly enhanced sensitivity is used to sense the test mass position. The sensor signal is fed back to a coil-magnet actuator to re-centre the test mass. The feedback for the AEI-accelerometers is processed using a real-time control and data system. The sensitivity of AEI-accelerometers is about 2.8×10^{-10} m s^{-2} $\mathrm{Hz}^{-1/2}$ at 1 Hz, which is close to the noise level of a Streckeisen STS-2 seismometer at 1.5×10^{-10} m s^{-2} $\mathrm{Hz}^{-1/2}$ at 1 Hz [22].

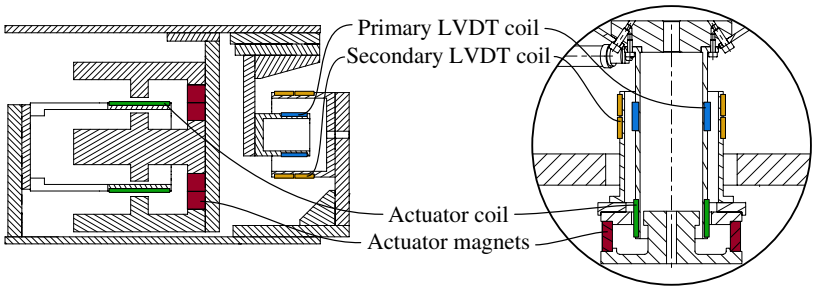

Figure 6. Schematic illustration of a horizontal (left) and a vertical (right) LVDT with their co-located actuators. The coils with the same function are indicated by the same colour. The circle on the right-hand side is a blow-up image of the GAS filter illustration (figure 3).

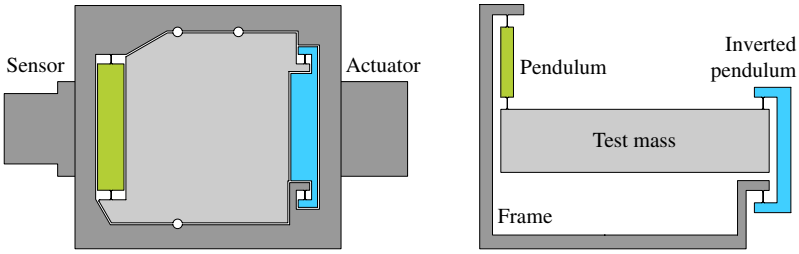

Figure 7. Schematic representation of the AEI-accelerometer (left). The position of the accelerometer's test mass (light grey) is measured by a miniaturized LVDT-sensor and is fed back to a voice-coil actuator which maintains centring of the mass. The right picture sketches the mechanical scheme of a folded pendulum (Watt-linkage). The left arm (green) a normal pendulum and the right (blue) an IP. All flexures are in tension to prevent buckling.

3.3. Vertical geophones

To monitor the residual vertical motion of the breadboard, three vertical geophones are installed within the honeycomb structure. These commercial geophones are model L-22D from Mark Products (now Sercel [23]). They have a natural frequency of 2 Hz and a sensitivity of 88 V $(\mathrm{m/s})^{-1}$. The geophones are not vacuum compatible, therefore they are sealed in air-tight tubes with ConFlat flanges. The tubes are filled with different marker gases to trace potential leaks.

Like most of the components in the AEI-SAS, three vertical geophones per table are distributed on a circle at 120° intervals. A simple geometry-inferred matrix transforms the signals of the three vertical geophones into the vertical and two rotational degrees of freedom within the control and data system.

3.4. Voice-coil actuators

Three vertical and three horizontal voice-coil actuators [24] are co-located with corresponding LVDTs, as shown in figure 6. The horizontal voice-coil actuators are placed close to the IP legs, actuating between the base plate and the spring box. They are positioned tangentially to a circle with 120° spacing. A coordinate transformation matrix is used to apply forces to the table in a Cartesian coordinate system. The vertical actuators are coaxial to each GAS filter,

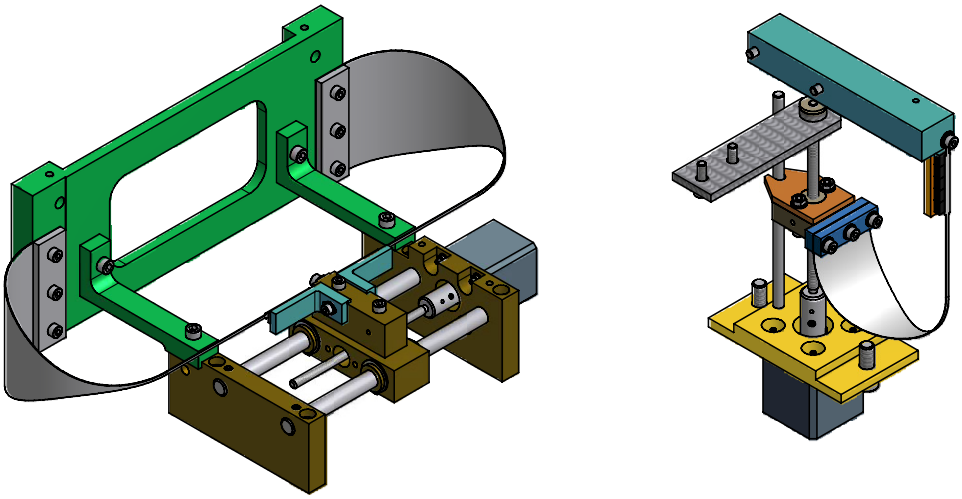

Figure 8. Motorized blade springs used in the AEI 10 m Prototype for fine corrections of table position. Three horizontal (left) and four vertical (right) springs are controlled by vacuum compatible stepper motors.

actuating between the keystone and the spring box. The horizontal actuators provide a force per unit current of 5 N A^{-1}. Vertical actuators, with about 7 N A^{-1}, are slightly stronger.

3.5. Motorized blade springs

Motorized springs driven by stepper motors are installed for static fine tuning of AEI-SAS position and for thermal drift compensation. Different sets of blades (see figure 8) are used to correct the static position of the table in vertical and horizontal degrees of freedom so that after mass re-distribution, the tables can be re-positioned at the original relative orientation to each other, by using a reference measurement. The tips of the spring blades are connected to a sliding carriage moved by a threaded rod attached to a stepper motor.

The thickness of the CuBe blade springs is 0.25 mm. The horizontal blades have been sized up in order to cope with ± 1 mrad misleveling of the IP base. The outline of the blade is designed to orient the resulting force along the movement direction. Three horizontal pairs of blades are positioned near each IP leg, actuating between the base plate and the spring box. Four vertical single blades, one at each corner of the optical table, act on the optical table from the spring box.

All motorized blades are driven by stepper motors of the type C17.2 from Arun Microelectronics Limited controlled by driver units IDX 7505 from Trinamic Motion Control. The stepper motors are vacuum compatible up to 10^{-10} mbar and bakeable to 200 °C. The motors are two-phase hybrid stepper motors, with side length of $31 \times 31 \times 41$ mm^3 and a torque rate of 0.2 Nm. Each motor has a step angle of 1.8° providing 200 full steps per revolution [25].

4. Table control strategy

Even though the tables are in close proximity, there will inevitably be some residual differential motion between them. The relative motion of these tables will be stabilized by a suspension

platform interferometer (SPI) composed by a set of Mach–Zehnder interferometers [26]. With this SPI, the position and orientation of the tables will be stabilized in all degrees of freedom, except roll about the optical axis of the SPI, via feedback to the voice-coil actuators.

The control and data taking for the AEI-SAS will be carried out with a dedicated digital system. All relevant servo loops will be implemented using the digital real-time control and data acquisition system, which is tested in view of its use for next generation gravitational wave detectors [27]. Control algorithms can be implemented via Matlab/Simulink models or C-code from which a real-time capable module is subsequently generated.

At the time of writing, the central AEI-SAS table and the South-table are already operational. The third AEI-SAS, carrying the West-table, will be assembled during the course of the years 2012/2013. This table will be used as a test-bed for improvements of the first two AEI-SAS tables. The SPI will be installed and tested on the first two tables. Subsequent publications describing the performance of the AEI-SAS and the SPI are planned.

Acknowledgments

The authors would like to thank the IMPRS for Gravitational Wave Astronomy and the Excellence Cluster QUEST (Centre for Quantum Engineering and Space-Time Research) for financial support.

References

[1] Dahl K *et al* 2012 Status of the AEI 10 m prototype *Class. Quantum Grav.* **29** 145005
[2] Lück H *et al* 2010 The upgrade of GEO 600 *J. Phys.: Conf. Ser.* **228** 012012
[3] Abernathy M *et al* 2011 *Einstein Gravitational Wave Telescope Conceptual Design Study (St. Stefano a Macerata—Cascina (PI), Italy, European Gravitational Observatory via E Amaldi)* http://dl.dropbox.com/u/18549909/et-design-study.pdf
[4] Müller-Ebhardt H *et al* 2008 Entanglement of macroscopic test masses and the standard quantum limit in laser interferometry *Phys. Rev. Lett.* **100** 013601
[5] Gräf C *et al* 2012 Optical layout for a 10 m Fabry–Pérot Michelson interferometer with tunable stability *Class. Quantum Grav.* **29** 075003
[6] Plissi M V *et al* 2000 GEO 600 Triple pendulum suspension system: seismic isolation and control *Rev. Sci. Instrum.* **71** 2539–45
[7] Stochino A *et al* 2009 The seismic attenuation system (SAS) for the advanced LIGO gravitational wave interferometric detectors *Nucl. Instrum. Methods* A **598** 737–53
[8] Accadia T *et al* 2012 Advanced Virgo technical design report *Virgo Technical Documentation System* VIR-0128A-12 https://tds.ego-gw.it/ql/?c=8940
[9] Robertson N *et al* 2004 Seismic isolation and suspension systems for Advanced LIGO *Proc. SPIE* **5500** 81–91
[10] Bertolini A *et al* 1999 Seismic noise filters, vertical resonance frequency reduction with geometric anti-springs: a feasibility study *Nucl. Instrum. Methods* A **435** 475–83
[11] Mantovani M *et al* 2005 One hertz seismic attenuation for low frequency gravitational waves interferometers *Nucl. Instrum. Methods* A **554** 546–54
[12] Stochino A *et al* 2007 Improvement of the seismic noise attenuation performance of the Monolithic Geometric Anti-spring filters for gravitational wave interferometric detectors *Nucl. Instrum. Methods* A **580** 1559–1564
[13] Sannibale V *et al* 2008 Recent results of a seismically isolated optical table prototype designed for Advanced LIGO *J. Phys.: Conf. Ser.* **122** 012010
[14] Takamori A *et al* 2007 Inverted pendulum as low frequency pre-isolation for advanced gravitational wave detectors *Nucl. Instrum. Methods* A **582** 683–92
[15] Losurdo G 1998 Ultra-low frequency inverted pendulum for the VIRGO test mass suspension *PhD Thesis* Pisa University, Pisa, Italy
[16] Tariq H *et al* 2002 The linear variable differential transformer (LVDT) position sensor for gravitational wave interferometer low-frequency controls *Nucl. Instrum. Methods* A **489** 570–576
[17] National Instruments tutorial 2006 Measuring position and displacement with LVDTs http://zone.ni.com/devzone/cda/tut/p/id/3638

[18] Bertolini A *et al* 2006 Readout system and predicted performance of a low-noise low-frequency horizontal accelerometer *Nucl. Instrum. Methods* A **564** 579–86
[19] Winterflood J 2001 High performance vibration isolation for gravitational wave detection *PhD Thesis* University of Western Australia, Crawley, Australia
[20] DeSalvo R 2009 Review: accelerometer development for use in gravitational wave-detection interferometers *Bull. Seismol. Soc. Am.* **99** 990–997
[21] Bertolini A *et al* 2006 Mechanical design of a single-axis monolithic accelerometer for advanced seismic attenuation systems *Nucl. Instrum. Methods* A **556** 616–23
[22] Nakayama Y *et al* 2004 Performance test of STS-2 seismometers with various data loggers *Proc. 8th Int. Workshop on Accelerator Alignment (CERN, Geneva)* eConf C04-10-04.11 041 www.slac.stanford.edu/econf/C04100411
[23] Sercel www.sercel.com/Company/history.php
[24] Wang C *et al* 2002 Constant force actuator for gravitational wave detector's seismic attenuation systems (SAS) *Nucl. Instrum. Methods* A **489** 563–9
[25] Arun Microelectronics Ltd. www.arunmicro.com/techdocs/datasheets/Stepper_motors.pdf
[26] Dahl K *et al* 2012 Suspension platform interferometer for the AEI 10 m prototype: concept, design and optical layout *Class. Quantum Grav.* **29** 095024
[27] Bork R 2010 AdvLIGO CDS design overview *Public LIGO Document Control Center* T0900612-v2 https://dcc.ligo.org/cgi-bin/DocDB/ShowDocument?docid=7834